Accuracy of Form Factors Used in Illuminating Engineering Radiosity Simulations

Gladimir V. G. Baranoski Jon G. Rokne

Department of Computer Science, The University of Calgary
2500 University Dr., N.W., Calgary, AB, T2N 1N4, Canada
E-mail: [gbaranos|rokne]@cpsc.ucalgary.ca

1 Introduction

The radiosity method is a valuable engineering tool that can be used to determine whether a lighting design meets project specifications. As mentioned by Ashdown [3], this method has appeared in the illuminating engineering literature as "radiative transfer theory" since the 1920s [28]. Recently, numerical linear algebra aspects directly associated with its practical application in illuminating engineering simulations have been investigated more closely by researchers from the lighting community [9, 18, 19].

The computation of form factors, which specify the fraction of radiation flux that leaves one surface and arrives at another, is central to the radiosity method. The errors introduced by form factor computation directly affect the correctness of the radiosity solutions, and may also slow down the convergence of the iterative methods used to solve radiosity systems. In this paper we investigate the errors introduced by different approaches used to compute form factors, aiming at the development of strategies to reduce their deleterious effects on the accuracy and efficiency of illuminating engineering simulations.

Several numerical methods are available for the computation of form factors. Generally speaking, these methods can be divided into two groups: deterministic and nondeterministic. In order to select one these methods, efficiency and accuracy criteria are taken into account. For off-line computations of form factors accuracy becomes the main criterion. As examples of applications in which form factors are usually computed off-line we can cite walkthroughs [25], sun and shade simulations [12], and radiative transfer studies in vegetation [7].

Initially, we examine the effects of the errors introduced by the numerical computation of form factor on the two properties of the radiosity coefficient matrix which are directly associated with the convergence of the iterative methods, namely its nonsingularity and its diagonal dominance. Besides this theoretical analysis, we compare the accuracy of two methods representing the deterministic and nondeterministic approaches usually applied to compute form factors. With these comparisons we highlight some important aspects that affect the accuracy of these approaches and discuss the differences in the magnitude and in the distribution of the errors introduced by each approach. Finally, we propose alternatives to minimize errors in the form factors and, consequently, improve the accuracy and efficiency of illuminating engineering simulations involving the radiosity method.

The remainder of this paper is organized as follows. Section 2 describes the radiosity system of linear equations and the formulation of the equation for the form factor between finite surfaces. Section 3 outlines the implications of the errors introduced during form factor computation. Section 4 describes the two methods used for the comparisons and Section 5 presents the criteria used to compare the accuracy of these methods. Section 6 discusses the results of these comparisons. The paper closes with a summary of the main conclusions and directions for future work.

2 Radiosity Background

2.1 Radiosity Equation

Assuming a closed environment whose surfaces are divided into n patches, the total spectral radiant flux leaving a patch depends on the spectral radiant flux emitted by the patch plus the spectral radiant flux that is reflected from the patch. The spectral radiant flux depends, in turn, on the total spectral radiant flux leaving the other patches in the environment. If we consider only the Lambertian[1] reflective behavior of these surfaces, we can drop the directional and positional dependencies on the spectral measures of light. In this case the process of spectral radiant flux transfer in a closed environment can be represented by:

$$\Phi_j(\lambda) = \Phi_j^E(\lambda) + \rho_j(\lambda) \sum_{i=1}^{n} F_{ij} \Phi_i(\lambda) \quad \textit{for } j = 1, 2 \ldots n \qquad (1)$$

where:

$\Phi_j(\lambda)$	=	total spectral radiant flux leaving patch j,
$\Phi_j^E(\lambda)$	=	spectral radiant flux emitted by patch j,
$\rho_j(\lambda)$	=	reflectance of patch j,
F_{ij}	=	form factor between patch i and patch j,
$\Phi_i(\lambda)$	=	total spectral radiant flux leaving patch i.

Since we are considering only the Lambertian reflective behavior of the surfaces in the environment, the process of radiant flux transfer only includes diffuse BRDFs[2] which are given by:

$$f_d(\lambda) = \frac{\rho_j(\lambda)}{\pi} \qquad (2)$$

In this case the reflectance $\rho_j(\lambda)$ represents the fraction of incident radiant flux which is reflected back to the environment at wavelength λ by a patch j, and π is incorporated in the definition of the form factor F_{ij}.

2.2 Form Factors

The form factor F_{ij}, also called configuration factor, indicates how a patch i "sees" a patch j. In other words, it specifies the fraction of radiant flux that leaves patch i and arrives at patch j. Form factors depend on the shape and relative orientation of the patches as well as on the presence of obstacles between them, which is indicated by the visibility term $V(x_i, x_j)$. The form factor F_{ij} between a patch i and a patch j (Figure 1) can be determined using the following expression:

[1] Ideal diffuse or Lambertian surfaces, such as chalk, appear equally bright from all viewing angles because they have a constant spectral radiance at all viewing angles under steady lighting conditions [22].

[2] A BRDF (*bidirectional reflectance distribution function*) is used to describe the spatial distribution of the reflected light [17].

$$F_{ij} = \frac{1}{A_i} \int_{A_i} \int_{A_j} \frac{cos\theta_i \; cos\theta_j}{\pi \|\vec{l_{ij}}\|^2} \; V(x_i, x_j) \; dA_i \; dA_j \qquad (3)$$

where:

A_i	=	area of patch i,
$\vec{l_{ij}}$	=	vector connecting a point x_i on patch i to a point x_j on patch j,
θ_i	=	angle between the vector $\vec{l_{ij}}$ and the normal of patch i,
θ_j	=	angle between the vector $\vec{l_{ij}}$ and the normal of patch j,
dA_i	=	differential area surrounding on patch i,
dA_j	=	differential area surrounding on patch j,
$V(x_i, x_j)$	=	visibility term.

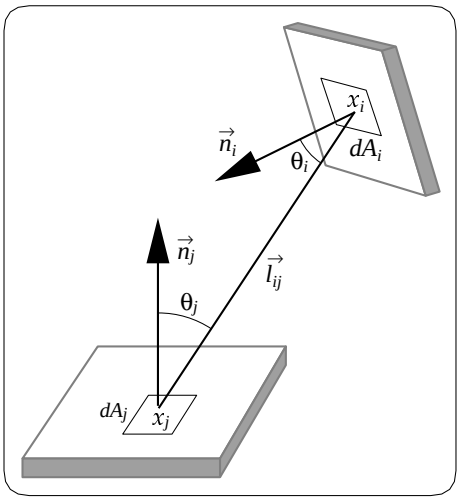

Figure 1: Geometry of the form factor between two patches.

Although there is in general no closed form solution for Equation 3, there are useful analytical formulae for simple geometrical configurations [21, 24, 26, 27]. These formulae are, however, usually not general enough to be used in global illumination[3]. For this reason, several numerical algorithms have been developed to compute form factors. As mentioned before, the numerical algorithms to compute form factors can be divided into two groups: deterministic, based on quadrature methods, and nondeterministic, based on Monte Carlo methods.

The computational costs involved in the computation of form factors can be reduced through the application of the following identities:

- Reciprocity relationship:

$$A_i F_{ij} = A_j F_{ji} \qquad (4)$$

- Summation relationship:

$$\sum_{j=1}^{n} F_{ij} \leq 1 \quad for \; i = 1, 2...n \qquad (5)$$

If we assume a closed environment, the above sum is by definition equal to 1.0. However, in practice, even for closed environments the computed value can be greater than 1.0 depending on the accuracy of the method used to compute the form factors.

- A planar or a convex patch can not see itself, which means that the form factor of a planar or a convex surface with respect to itself itself is:

$$F_{ii} = 0$$

However, there may be situations in which it may be appropriate to consider the form factor F_{ii} of a plane or convex patch different from zero. For example, suppose patches i and j are placed in front of each other and patch j is a perfect reflector[4] (mirror). In this case patch i can "see" itself and F_{ii} is different from zero.

- Finally, a concave patch can see itself, hence:

$$F_{ii} \neq 0$$

for this case.

2.3 Radiosity System of Equations

Sometimes it is more convenient to rewrite Equation 1 in terms of spectral radiant exitance and spectral irradiance [1]. The first of these terms refers to the total spectral radiant flux leaving an element per unit of area and the second term refers to the spectral radiant flux emitted by an element per unit of area. In this case, from [22], we have:

$$\Phi_j(\lambda) = \pi M_j(\lambda) A_j \qquad (6)$$

where:

$M_j(\lambda)$	=	spectral radiant exitance of patch j,
A_j	=	area of patch j.

Also from [22], we have:

$$\Phi_j^E(\lambda) = \pi E_j(\lambda) A_j \qquad (7)$$

where:

$E_j(\lambda)$	=	spectral irradiance emitted from patch j.

Substituting Equation 6 and Equation 7 into Equation 1 gives:

$$\pi M_j(\lambda) A_j = \pi E_j(\lambda) A_j + \rho_j(\lambda) \sum_{i=1}^{n} F_{ij} \, M_i(\lambda) A_i \qquad (8)$$

$for \; j = 1, 2...n.$

Applying the form factor reciprocity relationship (Equation 4) in Equation 8 and dividing it by A_j we get:

$$\pi M_j(\lambda) = \pi E_j(\lambda) + \rho_j(\lambda) \sum_{i=1}^{n} \pi F_{ji} M_i(\lambda) \qquad (9)$$

$for \; j = 1, 2...n.$

Dividing the above expression by π, we finally get the classical expression in terms of spectral radiant exitance, which holds for each patch in the environment:

$$M_j(\lambda) = E_j(\lambda) + \rho_j(\lambda) \sum_{i=1}^{n} F_{ji} M_i(\lambda) \qquad (10)$$

[3] The problem of determining the appearance of an environment by simulating the transport of light within it, which includes the problems of light emission, propagation, scattering and absorption, is known as global illumination [2, 25].

[4] Usually non-Lambertian surfaces are not introduced in a radiosity system. Their effects on the form factors of the surrounding Lambertian surfaces can, however, be accounted for through the use of extended form factors [8, 20].

$for\ j = 1, 2...n.$

In the thermal engineering and computer graphics literatures the term radiosity is used to refer to radiant exitance. For the sake of consistency with the standard illumination engineering literature [1], we will continue to use the term radiant exitance throughout this paper when refering to the radiant flux density leaving a surface or patch. Moreover, in order to simplify matters, we are going to suppress the dependence on wavelength in the next expressions.

In order to determine the radiant exitance of each patch of a given environment we need to solve a system of linear equations whose coefficient matrix we denote by G. The vector of unknowns of this system is represented by the vector of radiant exitances m and the right-hand side vector of this system is represented by the vector of irradiances e. This radiative transfer system, also known as the radiosity system, is represented as:

$$Gm = e \tag{11}$$

where the elements of G are $G_{ij} = \delta_{ij} - \rho_i F_{ij}$ (with δ_{ij} being the Kronecker delta). The coefficient matrix G, also known as the radiosity coefficient matrix, is commonly represented by:

$$G = I - PF \tag{12}$$

where:

I	=	identity matrix,
P	=	diagonal matrix whose diagonal entries p_{ii} correspond to ρ_i,
F	=	form factor matrix.

Direct methods for solving linear systems, such as Gaussian Elimination [6] or LU decomposition [6], are not suitable for large radiosity systems of equations because of the relative low density of the coefficient matrix and because rapid solutions at relatively low accuracy are needed. These aspects plus the special properties of the radiosity coefficient matrix, namely its nonsingularity[5] and diagonal dominance[6], make the use of iterative methods more convenient. These methods are generally of the following form:

```
1  initialize m and r
2  while (not converged)
3        select ∇m
4        update m = m + ∇m
5        update r = r − G∇m
```

where ∇m corresponds to the correction vector and r corresponds to the residual vector given by:

$$r = e - Gm \tag{13}$$

The iterative methods used to solve the radiosity system of linear equations can be divided into general matrix methods and radiosity-specific methods. The methods that belong to the former group update all components of the solution vector on each iteration, *e.g.*, the conjugate gradient and the Chebyshev methods [5]. The methods that belong to the latter group update a single component on each iteration, *e.g.*, progressive refinement and overshooting methods. The expression *radiosity-specific methods*, used in the computer graphics literature, is applied to group methods specifically developed to solve the radiative transfer system described above [5]. Although those methods can be considered variations of numerical methods, such as Southwell Iteration [10] or SOR [6], they have been adjusted and fine-tuned to the radiant exitance case.

3 Implications of the Errors Introduced in the Numerical Computation of Form Factors

From the discussion presented above, it is clear that the errors introduced in the form factor computation affect the radiant exitance vector m. Recall that to obtain this vector we must solve, either explicitly or implicitly, the radiosity system given by $Gm = e$ (Section 2.3) whose coefficient matrix G is given by $I - PF$.

Besides the effect mentioned above, these errors may have other subtle effects, with possibly larger implications for the accuracy of radiosity solutions. Recall that the selection of iterative methods to solve the radiosity system of linear equations was based on two general assumptions, namely the diagonal dominance and the nonsingularity of G. Although, in theory, these properties hold for radiosity systems, it may not be the case in practice.

If the errors introduced in the computation of the form factors for a given surface of the environment are such that their summation relationship (Equation 5) does not hold anymore, then we cannot ensure the diagonal dominance of G (Section 2.3). Moreover, we cannot guarantee that $\varrho(PF)$, the spectral radius[7] of PF, be less than 1. In this case, Theorem 4.4 of Young [29] (page 35), adapted to the radiative transfer notation, states that:

> If $\varrho(PF) < 1$ then G is nonsingular and the series $I + PF + (PF)^2 + \cdots$ converges to G^{-1}. Conversely, if $\varrho(PF) \geq 1$ then the series does not converge, and it cannot be guaranteed that G^{-1} exists.

Thus we cannot ensure the nonsingularity of G either.

The failure to fulfill the diagonal dominance property makes the iterative process more time consuming. This happens because, in this case, we need to apply techniques, such as pivoting [11], to enforce this property. The failure to fulfill the nonsingularity property has, however, a more serious consequence. In this case the convergence of the iterative methods cannot be guaranteed at all.

4 Statement of Methods

The Parametric Differential Method (PDM) [4] is an example of a deterministic method for form factor computation between two surfaces or patches. This method evaluates the integrand of Equation 3 using a numerical technique called Gaussian quadrature [6]. Points of evaluation, or nodes[8], are placed in both patches according to the roots of Legendre polynomials [6] (Figure 2). The value of the visibility term $V(x_i, x_j)$ (Section 2.2) is determined by testing the intersection of rays, which connect pairs of nodes, with other objects in the environment. For example, when one uses a 5-points Gaussian quadrature 25 nodes are placed on each patch and 625 rays are used to test for obstacles between the two patches.

One of the nondeterministic methods for form factor computation uses the ray casting technique [3, 16] and, although it can be extended to specular (non-Lambertian) surfaces, it is usually applied to diffuse (Lambertian) surfaces [23]. In order to compute the form factor between diffuse patches a set of sample points is randomly distributed in a source patch and rays are shot from these sample points in random directions having a cosine distribution (Figure 3). The number of times each patch in the environment is hit by a ray

[5] An $n \times n$ matrix K is said to be nonsingular if an $n \times n$ matrix K^{-1} (the inverse of K) exists such that $KK^{-1} = K^{-1}K = I$ [6]. Alternatively a matrix K is also said to be nonsingular if its determinant is nonzero [15].

[6] Assuming that $0 \leq \rho < 1$ and that the sum of form factors in any row is equal to one, we can say that the matrix G is strictly diagonally dominant, since the property $|G_{ii}| > \sum_{\substack{j=1 \\ j \neq i}}^{n} |G_{ij}$ holds for each $j = 1, 2, \ldots, n$.

[7] The spectral radius $\varrho(K)$ of a matrix K is defined by $\varrho(K) = max \mid \Lambda \mid$, where Λ is an eigenvalue of K [6].

[8] These points of evaluation can also be called sample points. For the sake of consistency with the numerical analysis literature, we will use the term node when referring to deterministic procedures used to compute form factors.

is recorded. Using this approach the form factor between a source patch i and a patch j is given by the number of rays that hit patch j divided by the total number of rays shot from patch i. Henceforth we will refer to this method as SR, *i.e.*, shooting method with a random distribution of sample points.

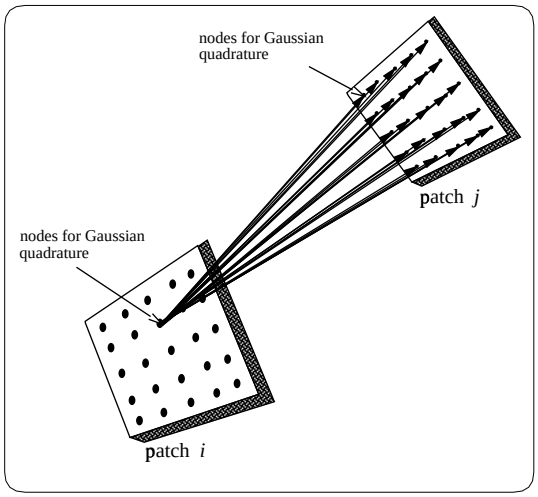

Figure 2: Geometry for a deterministic method for form factor computation using Gaussian quadrature.

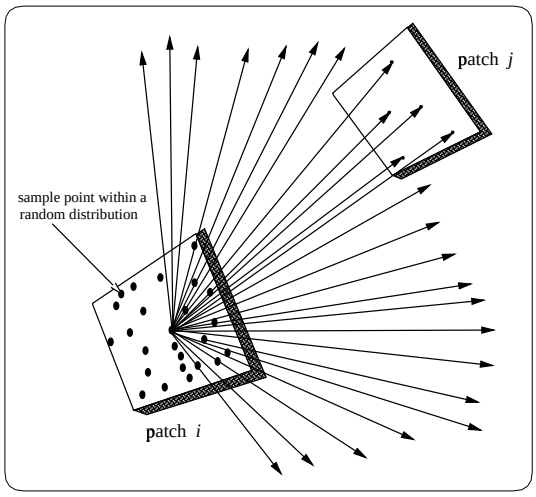

Figure 3: Geometry for a nondeterministic method for form factor computation using a random distribution of sample points.

5 Comparison Criteria

In order to evaluate the accuracy of numerical methods for form factor computations it is convenient to use geometries for which the analytical form factors are available to be used as reference. In the tests performed in this paper we considered an environment formed by a cube, or box (Figure 4), which allow us to fulfill this evaluation guideline. Recall that the summation of the form factors of one surface or patch with respect to the other surfaces or patches of a closed environment must be equal to 1.0 (Equation 5). We use this summation relationship as well as the analytical form factors for parallel and perpendicular surfaces to evaluate the accuracy of the results provided by both methods regarding the test environment.

The analytical form factor for parallel, directly opposed patches or surfaces, such as faces 1 and 6 (Figure 4), is given by the following expression presented by Hamilton and Morgan [13] and Hottel [14]:

$$\begin{aligned} F_{1-6} = \; & \frac{2}{\pi XY}\left\{ ln\left[\frac{(1+X^2)(1+Y^2)}{1+X^2+Y^2}\right]^{\frac{1}{2}}\right. \\ & +X\sqrt{1+Y^2}\;tan^{-1}\left(\frac{X}{\sqrt{1+Y^2}}\right) \\ & +Y\sqrt{1+X^2}\;tan^{-1}\left(\frac{Y}{\sqrt{1+X^2}}\right) \\ & \left.-X\;tan^{-1}(X)-Y\;tan^{-1}(Y)\right\} \end{aligned} \tag{14}$$

where X and Y are given by:

$$X = \frac{a}{c} \tag{15}$$

$$Y = \frac{b}{c} \tag{16}$$

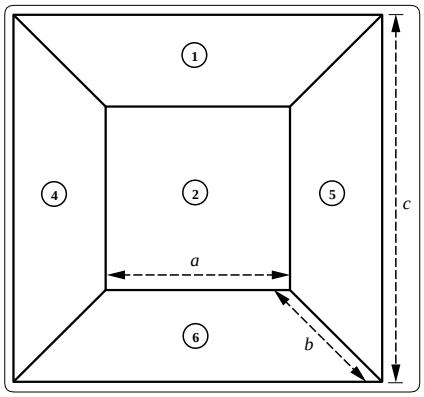

Figure 4: Sketch of the test environment (face 3 is frontal).

The analytical form factor for two patches or surfaces of same length, having a common edge, and at angle of 90° to each other, such as the faces 1 and 2 (Figure 4), can be obtained through a similar expression provided by Hottel [14] and Hamilton and Morgan [13]. Alternatively, assuming that the form factor between the analytical parallel faces have already been computed and using the summation relationship of the form factors, the analytical form factor for perpendicular surfaces, such as faces 1 and 2, can be obtained through the following expression:

$$F_{1-2} = \frac{1 - F_{1-6}}{4} \tag{17}$$

In the tests presented in this paper we considered the dimensions of the cube presented in Figure 4 given by $a = b = c = 6.0$. Replacing these values in the Equation 14, the analytical form factor for the parallel faces of the cube is equal to 0.199824. Replacing this value in the Equation 17, the analytical form factor for the perpendicular faces of the cube is equal to 0.200043. For the sake of simplicity, all the figures for analytical and numerical form factors presented in this paper were truncated after the sixth digit. Moreover, in order to determine the relative error regarding the summation relationship for each individual face and the form factors for the different pairs of faces we used the following expression:

$$r.e.\;(\%) \;=\; \frac{|analytical\;value \;-\; numerical\;value|}{|analytical\;value|} \tag{18}$$

6 Results and Discussion

Intuitively we may consider that the accuracy of both methods can be increased by subdividing the faces into a larger number of patches. Table 1 shows the effects of finer surface subdivisions on the accuracy of the form factors computed using the PDM. In this experiment we used 25 nodes per patch and 25 rays per node. As we can see, there is a direct relationship between the increase in the number of patches and the increase on the accuracy of the form factors computed using the PDM.

	number of patches		
	216	486	1014
Σ of face l	1.013652	1.009103	1.006303
Σ of face 2	1.013652	1.009103	1.006303
Σ of face 3	1.013652	1.009103	1.006303
Σ of face 4	1.013652	1.009103	1.006303
Σ of face 5	1.013652	1.009103	1.006303
Σ of face 6	1.013652	1.009103	1.006303
Σ of $r.e.$ (%)	8.19	5.46	3.78

Table 1: Effects of finer surface subdivisions on the accuracy of the PDM.

Such a direct relationship, however, cannot be always observed for nondeterministic methods as demonstrated by the figures presented in Table 2. This table shows the effects of finer surface subdivisions on the accuracy of the form factors computed using the SR. In this experiment we used 1000 sample points per patch and one ray per sample point.

	number of patches		
	216	486	1014
Σ of face l	1.0	1.0	1.0
Σ of face 2	0.997333	0.997815	1.00034
Σ of face 3	1.001140	1.0009	1.00208
Σ of face 4	0.998056	1.00023	0.999124
Σ of face 5	1.003670	1.00049	1.00108
Σ of face 6	1.004640	0.998506	0.995243
Σ of $r.e.$ (%)	2.43	0.53	0.91

Table 2: Effects of finer surface subdivisions on the accuracy of the SR.

Increasing the number of rays per source patch can also increase the accuracy of the form factors. Table 3 illustrates this aspect for an application of the SR (using 1000 sample points per patch and one ray per sample point) in which the test environment was divided into 54 patches.

	number of rays	
	10000	1000000
Σ of face l	1.0	0.999994
Σ of face 2	0.998789	0.999691
Σ of face 3	0.997356	0.999901
Σ of face 4	1.00064	0.999982
Σ of face 5	0.999844	0.999935
Σ of face 6	1.00197	1.00009
Σ of $r.e.$ (%)	0.66	0.0587

Table 3: Effects of higher ray densities on the accuracy of the SR.

In order to compare the accuracy of both methods, PDM and SR, we considered the test environment divided into 1014 patches (169 patches per face) and 625 rays per source patch. The results present in Table 4 seem to indicate that the nondeterministic method is more accurate than the deterministic method for the test environment used in our experiments. However, since the figures presented in this table correspond to summations, it may be possible that a cancellation of error terms occurs when we perform the sum of form factors regarding each individual face of the cube. This cancellation may, in turn, hide a higher accuracy provided by the deterministic method for certain geometries. Indeed, Table 5 shows that the deterministic method provides more accurate results than the nondeterministic method for form factors for pairs of parallel faces.

	method	
	PDM	SR
Σ of face l	1.006303	1.0
Σ of face 2	1.006303	1.00016
Σ of face 3	1.006303	0.97264
Σ of face 4	1.006303	0.999451
Σ of face 5	1.006303	1.00034
Σ of face 6	1.006303	1.00235
Σ of $r.e.$ (%)	3.78	0.61

Table 4: Comparison between the PDM and the SR considering the environment divided into 1014 patches and using 625 rays per source patch.

F_{ij}	PDM	$r.e.$ (%)	SR	$r.e.$ (%)
1 - 6	0.199841	0.02	0.199044	0.38
2 - 3	0.199841	0.02	0.199044	0.38
4 - 5	0.199841	0.02	0.199195	0.30

Table 5: Form factors for the parallel faces divided into 169 patches each.

The accuracy of both methods is affected by the possibility of the integrand of Equation 3 [8] being close to singular, which may occur when the two differential areas are too close. When this occurs, the task of determining which method provides more accurate results becomes more difficult. Table 6 presents the relative errors for the form factors between the pairs of perpendicular faces. As we can see, only for two cases the relative errors for the form factors obtained using the nondeterministic method were greater than those regarding the deterministic method. Although this aspect may suggest that the random distribution of sample points used by the SR may be less prone to singularity problems, it does not guarantee a smaller error for all the cases due to the stochastic nature of the SR.

F_{ij}	PDM	$r.e.$ (%)	SR	$r.e.$ (%)
1 - 2	0.201615	0.78	0.200502	0.23
1 - 3	0.201615	0.78	0.200634	0.30
1 - 4	0.201615	0.78	0.199044	0.50
1 - 5	0.201615	0.78	0.200625	0.29
2 - 4	0.201615	0.78	0.198892	0.58
2 - 5	0.201615	0.78	0.201051	0.50
2 - 6	0.201615	0.78	0.200691	0.32
3 - 4	0.201615	0.78	0.200161	0.06
3 - 5	0.201615	0.78	0.198305	0.86
3 - 6	0.201615	0.78	0.199138	0.45
4 - 6	0.201615	0.78	0.202159	1.06
5 - 6	0.201615	0.78	0.201164	0.56

Table 6: Form factors for the perpendicular faces divided into 169 patches each.

7 Conclusion and Future Work

In this paper we discussed the implications of errors introduced in the computation of form factors and compared two different approaches used to perform these computations. For these comparisons we considered an environment for which the corresponding analytical form factors are available to be used as a reference.

The results of these comparisons show that, even for simple environments, such as the one used in our experiments, a single method cannot provide the most accurate results for all possible geometries. Usually, for geometries not prone to singularity problems, the deterministic methods may provide more accurate results. Moreover, while the error associated with the deterministic methods is uniform, the error associated with the nondeterministic methods is nonuniform. This aspect suggests that more sophisticated statistical analysis tools shall be brought to bear on future comparisons. As future work, we intend to extend our experiments to environments with occluded objects.

Finally, despite the simplicity of the environment used in our experiments, it was shown that selecting the "best" method is delicate since no single method is superior in all cases. The relative accuracy depends on the geometrical characteristics of the environment. Therefore, the development of accurate practical solutions for off-line computation of form factors will likely require implementing different methods with the application of a given method determined by the geometry at hand. For example, considering the environment used in our experiments, one could use the deterministic method for the parallel faces and the nondeterministic one for the perpendicular faces.

Acknowledgments

The authors would like to thank David Wilson at the University of Calgary for his helpful suggestions and the anonymous reviewers for their useful insights. The work presented in this paper was supported in part by CNPq (Proc. 200876/93-7, Brazil) and by NSERC (PDF 207026, Canada).

REFERENCES

[1] ANSI. Nomenclature and definitions for illuminating engineering. In *ANSI/IES RP-6-1986*. Illuminating Engineering Society of North America, New York, 1986.

[2] J. Arvo. *Analytic Methods for Simulated Light Transport*. PhD thesis, Yale University, 1995.

[3] I. Ashdown. *Radiosity: A programmers's perspective*. John Wiley & Sons, New York, NY, 1994.

[4] G. Baranoski. The parametric differential method: An alternative to the calculation of form factors. *Computer Graphics Forum (EUROGRAPHICS Proceedings)*, 11(3):193–204, September 1992.

[5] G. Baranoski, R. Bramley, and P. Shirley. Fast radiosity solutions for environments with high average reflectance. In P. M. Hanrahan and W. Purgathofer, editors, *Rendering Techniques'95 (Proceedings of the Sixth Eurographics Rendering Workshop)*, pages 345–356, Dublin, June 1995. Springer-Verlag.

[6] R. Burden and J. Faires. *Numerical Analysis*. PWS-KENT Publishing Company, Boston, fifth edition, 1993.

[7] M. Chelle, B. Andrieu, and K. Bouatouch. Nested radiosity for plant canopies. *The Visual Computer*, 14(3):109–125, 1998.

[8] M. Cohen and J. Wallace. *Radiosity and Realistic Image Synthesis*. Academic Press Professional, Cambridge, 1993.

[9] D. DiLaura and P. Franck. On setting up and solving large radiative transfer systems. *Journal of the Illuminating Engineering Society*, 22(2):3–7, October 1993.

[10] S. Goertler, M. Cohen, and P. Slusallek. Radiosity and relaxation methods. *IEEE Computer Graphics and Applications*, 14(6):48–58, November 1994.

[11] G. Golub and C. V. Loan. *Matrix Computations*. John Hopkins University Press, Baltimore, second edition, 1989.

[12] D. Greenberg. Computers and architecture. *Scientific American*, 264(2):104–109, February 1991.

[13] D. Hamilton and W. Morgan. Radiant-interchange configuration factors. Technical Report TN-2836, NASA, 1952.

[14] H. Hottel. Radiation heat transmission between surfaces separated by non-absorbing media. *Trans. ASME*, 53:265–273, 1931.

[15] P. Lancaster and M. Tismenetsky. *The Theory of Matrices*. Academic Press, San Diego, second edition, 1985.

[16] G. Maxwell, M. Bailey, and V. Goldschmidt. Calculations of the radiation configuration factor. *Computer-aided Design*, 18(7):371–379, September 1986.

[17] F. Nicodemus, J. Richmond, J. Hsia, I. Ginsberg, and T. Limperis. Geometrical considerations and nomenclature for reflectance. In L. Wolff, S. Shafer, and G. Healey, editors, *Physics-Based Vision Principles and Practice: Radiometry*, pages 94–145, Boston, 1992. Jones and Bartlett Publishers.

[18] Y. Nievergelt. Making any radiosity matrix symmetric positive definite. *Journal of the Illuminating Engineering Society*, 26(1):165–172, 1997.

[19] Y. Nievergelt. Radiosity in illuminating engineering. *The UMAP Journal*, 18(2):167–179, 1997.

[20] H. Rushmeier and K. Torrance. Extending the radiosity method to include specularly reflecting and translucent materials. *ACM Transactions on Graphics*, 9(1):1–27, January 1990.

[21] P. Schroder and P. Hanrahan. On the form factor between two polygons. In *SIGGRAPH Proceedings, Annual Conference Series*, pages 163–164, 1993.

[22] P. Shirley. *Physically based lighting for computer graphics*. PhD thesis, Dept. of Computer Science, University of Illinois, November 1990.

[23] P. Shirley. Radiosity via ray tracing. In *Graphics Gems II*, pages 306–310. Ed. Academic Press, 1991.

[24] R. Siegel and J. Howell. *Thermal Radiation Heat Transfer*. MacGraw-Hill Kogakusha, Tokyo, 1972.

[25] F. Sillion and C. Puech. *Radiosity and Global Illumination*. Morgan Kaufmann Publishers, San Francisco, 1994.

[26] E. Sparrow and R. Cess. *Radiation Heat Transfer*. Brooks/Cloe, Belmont, 1966.

[27] J. Wiebelt. *Engineering Radiation Heat Transfer*. Holt Rimehart and Winston, New York, 1966.

[28] Z. Yamauti. The light flux distribution of a system of interreflecting surfaces. *Journal of the Optical Society of America*, 13:561–571, November 1926.

[29] D. Young. *Iterative Solution of Large Linear Systems*. Academic Press Inc., New York, 1971.